The Sensitivity of the Outgoing Longwave Radiation to Surface Temperature: Modeling the Opacity Feedback and Experiments with a Variable Cloud-Top Temperature Provision

BINYAMIN U. NEEMAN, JOACHIM H. JOSEPH AND GEORGE OHRING*

Department of Geophysics and Planetary Sciences, Tel-Aviv University, Ramat-Aviv, Israel

(Manuscript received 22 September 1986, in final form 20 April 1987)

ABSTRACT

An efficient longwave scheme for climate models originally suggested by Sasamori is modified to correctly simulate the water vapor–temperature feedback mechanism. It is found that the modified scheme with a fixed cloud-top altitude (FCA) correctly simulates the longwave sensitivity to surface temperature, $\partial F^{\uparrow}/\partial T_s$, over the clear portion of the sky, but that over the cloud portion of the sky $\partial F^{\uparrow}/\partial T_s$ remains too high. The fixed cloud-top temperature (FCT) method is similarly reviewed and tested. Comparisons with observational Budyko-type correlations are shown to be indecisive over the question of FCA vs FCT.

A direct observational correlation between the effective cloud-top and surface temperatures, based on annually averaged cloud statistics data, suggests a variable cloud-top temperature (VCT) model. In such a model, the temperature of the effective cloud-top layer is varied according to changes in the surface temperature at a rate which is intermediate between that of the FCA and FCT models. This model results in a reasonable $\partial F^{\uparrow}/\partial T_s$ over the cloud portion of the sky.

The modified longwave scheme is implemented into a zonally averaged dynamic climate model. It is shown that when the VCT mechanism is invoked, climate sensitivity is doubled compared to that simulated with the FCA model. The importance of simulating not only the correct longwave flux, but also the correct longwave sensitivity to temperature changes is therefore stressed for radiation schemes in studies involved with climate change.

1. Introduction

It is of crucial importance in climate modeling, and in climate change experiments, in particular, that $\delta F^{\uparrow}/\delta T_s$,[1] the sensitivity of the outgoing longwave radiation $F^{\uparrow}$ to changes in the surface temperature T_s, be correctly simulated. The analysis of simple time-dependent energy balance models shows that the longwave sensitivity parameter $\delta F^{\uparrow}/\delta T_s$, in effect, determines their sensitivity to externally forced perturbations, their stability and their radiative relaxation time and response to cyclic or transient forcing (North et al., 1981).

Warren and Schneider (1979) have shown that uncertainties in the value of $\delta F^{\uparrow}/\delta T_s$ significantly influence the sensitivity and the stability of energy balance climate models. For example, for a particular ice albedo feedback experiment, they found that for $\delta F^{\uparrow}/\delta T_s = 1.37$ W m^{-2} °C^{-1}, a decrease of the solar constant by 6.5% was required to produce an ice-covered earth, while for $\delta F^{\uparrow}/\delta T_s = 2.25$ W m^{-2} °C^{-1}, a decrease of 21% was required. A similar result was obtained independently by Hartmann and Short (1979).

The outgoing longwave radiation $F^{\uparrow}$ is a function of the vertical distribution in the atmosphere of several variables (following Ohring and Gruber, 1984):

$$F^{\uparrow} = f[T(z), w_i(z), A_c(z)] \tag{1}$$

where z is the height, w_i the mixing ratio of the ith absorbing constituent (H_2O, CO_2, O_3, and aerosols) and A_c the cloud amount. Had the variables in Eq. (1) been well defined in terms of T_s, it would have been possible to calculate $\delta F^{\uparrow}/\delta T_s = df/dT_s$ using the chain rule of partial differentiation. However, this treatment is limited by the lack of a unique functional dependence between the variables. Wang et al. (1981) have suggested that A_c may not be related in a simple manner to either the surface temperature or the cloud feedbacks produced by climate variations. The cloud amount–temperature feedback mechanism is complicated by the competing albedo and greenhouse effects, the latter being dependent on the vertical distribution of cloud-cover changes and on the tropospheric lapse rate. A review and analysis of this subject is available in Ohring and Gruber (1984). The complexity of cloud feedbacks is further increased by variations in the cloud optical thickness (Wang et al., 1981) and by the interaction of the sides of the clouds in a broken-cloud field with each other and with the ground (Harshvardhan and Weinman, 1982).

The present study is concerned with two feedback mechanisms affecting the longwave sensitivity $\delta F^{\uparrow}/\delta T_s$,

* Present affiliation: NESDIS/NOAA, Washington, D.C. 20233.

[1] The use of the "virtual differential" $\delta F^{\uparrow}/\delta T_s$ instead of the "real differential" $dF^{\uparrow}/dT_s$ emphasizes the nonuniqueness of the differential and is subsequently justified.

one connected with variations in the water vapor optical path and the other with cloud-top height changes. The water vapor–surface temperature coupling is a positive feedback mechanism, since an increase in T_s is associated with an increase in temperature in the atmosphere and a rise in its ability to hold water vapor, such that the relative humidity remains approximately constant (Manabe and Wetherald, 1967), thus increasing the atmospheric longwave opacity with a subsequent increase in surface temperature. The water vapor–temperature feedback has been tested in radiative transfer model simulations in which the relative humidity r, the lapse-rate γ and cloud amount A_c were held constant, yielding a value of $\delta F^{\uparrow}/\delta T_s = (\partial F^{\uparrow}/\partial T_s)_{r,\gamma,A_c}$ between 2.0 W m^{-2} °C^{-1} (Cess, 1974) and 2.2 W m^{-2} °C^{-1} (Ramanathan et al., 1976), with increases of 0.2–0.4 W m^{-2} °C^{-1} over the cloud portion of the sky in both cases.

The cloud-top–surface temperature coupling is a positive feedback mechanism with similar effect. Provided an increase in T_s is responsible for an increase in the cloud-top altitude, as argued in the present study, the cloud-top temperature would experience a smaller increase than T_s, or, at the extreme condition, remain fixed. The effect is a smaller increase in $F^{\uparrow}$ with subsequent increase in T_s. A comparison of their results with the semiempirical results of Budyko (1969) has led Cess (1974) and Ramanathan et al. (1976) to suggest a *fixed cloud-top temperature* (FCT) model, which they claimed to be advantageous over the more standard *fixed cloud-top altitude* (FCA) model, especially for the modeling of climate change, since the FCT model seemed to simulate more accurately the longwave sensitivity, particularly over the cloud portion of the sky. The FCT approach is discussed in detail later, and its results are compared with new observations.

During the last decade, there have been a number of observational studies using radiation measurements from satellites, where $F^{\uparrow}$ has been correlated with T_s, A_c and sometimes with the product term $A_c \cdot T_s$. These studies have employed different sampling techniques and satellite data. For a comprehensive review of these studies, see Ohring and Gruber (1984). The estimate of $\delta F^{\uparrow}/\delta T_s$ from these observational studies is in the range 1.90 ± 0.35 W m^{-2} °C^{-1}. The observational study of Short et al. (1984) has demonstrated possibly large spatial–time deviations from the above estimate of $\delta F^{\uparrow}/\delta T_s$, mainly in regions with large seasonal variations in cloud amount.

In the present study, an efficient simplification for longwave radiation schemes originally suggested by Sasamori (1970) for the use in climate models and GCMs is tested and modified in section 2 to correctly simulate the water vapor–temperature or opacity feedback mechanism. Section 3 deals with the FCT model approach, and a more realistic *variable cloud-top temperature* (VCT) model is suggested. Due to uncertainties in the cloud feedback mechanisms described above, no attempt is made in the present study to model the response of the cloud *amount* to temperature changes. As mentioned previously, this feedback is weakened due to the competing albedo and greenhouse effects. It may nevertheless be worthwhile to focus on this cloud amount feedback in future study. In section 4 the modified longwave scheme is verified and the VCT model evaluated utilizing a climate model version of the hemispheric dynamic zonally averaged model of Ohring and Adler (1978, 1980) (hereafter referred to as OA).

2. The longwave radiation scheme

Sasamori (1970) has presented a simplified method of longwave radiation flux calculation, eliminating the time-consuming calculations of the absorptivity functions. His method has traditionally been used in NCAR GCMs (see Kasahara and Washington, 1971) and has also been employed in OA. It will be shown later that by the use of prescribed "mean source functions", Sasamori's simplification underestimates the effect of the opacity feedback mechanism.

The following is a discussion of Sasamori's simplification for the outgoing longwave radiation at the top of the atmosphere over the clear portion of the sky, $F^{\uparrow}_{\text{clear}}$, checking its sensitivity to changes in the surface temperature, T_s. $F^{\uparrow}_{\text{clear}}$ is given in Sasamori (1970) by

$$F^{\uparrow}_{\text{clear}} = \sigma \langle T \rangle_A{}^4 \bar{A}_0(u_A) + \sigma T_s^4 [1 - \bar{A}_0(u_A)] \qquad (2)$$

where u_A is the effective pathlength of the atmosphere, $\bar{A}_0$ the "average absorptivity" for the range of temperature from 30° to −50°C (Sasamori, 1968), σ the Stefan-Boltzmann constant and $\langle T \rangle_A$ the "mean source function" representing the effective temperature of the atmosphere and is given by

$$\left.\begin{aligned} \langle T \rangle_A{}^4 &= \frac{\int_0^{z_t} w_A(z,z') T^4 dz'}{\int_0^{z_t} w_A(z,z') dz'} \\ w_A(z,z') &= \exp[-|z-z'|/D_A(z)] \end{aligned}\right\}, \qquad (3)$$

where $D_A(z)$ is a scale length representing the effective thickness of the emission layer (Table 1 of Sasamori, 1970).

Partial differentiation of (2), holding the relative humidity r and the lapse-rate γ constant, gives

$$\frac{\partial F^{\uparrow}}{\partial T_s} = \sigma \bar{A}_0 \frac{\partial \langle T \rangle_A{}^4}{\partial T_s} + \sigma \langle T \rangle_A{}^4 \frac{\partial \bar{A}_0}{\partial T_s} + \sigma \frac{\partial T_s^4}{\partial T_s}[1 - \bar{A}_0] - \sigma T_s^4 \frac{\partial \bar{A}_0}{\partial T_s}. \qquad (4)$$

The actual value of each of the terms in (4) was found in the present study by assuming a standard atmosphere with $T_s = 288$ K, $\gamma = 6.5$°C km^{-1}, $r = 0.75$, a vertical

TABLE 1. Comparison of the values (in W m^{-2} °C^{-1}) of each of the terms in Eq. (4), with Sasamori's simplified method and with the new longwave scheme.

Method	$\left(\frac{\partial F^{\uparrow}}{\partial T_s}\right)_{r,\gamma}$	=	Term 1	+	Term 2	+	Term 3	+	Term 4
Sasamori (1970)	2.61		2.11		0.65		1.39		−1.52
New scheme	2.22		1.54		0.79		1.40		−1.51

distribution of specific humidity according to $q = q_s(p/p_s)^{\lambda}$ where $\lambda = 3.0$ (subscript s refers to surface values), a tropopause at $z = 13$ km, and by letting $\Delta T_s = +1$°C.

Next, the calculation was repeated with a modified longwave scheme. The modified scheme integrates the standard "radiation chart" transfer equations, without making use of Sasamori's (1970) simplification and without approximating the absorptivity $\bar{A}(u, T)$ for water vapor by $\bar{A}_0$. Its details (appendix A) may be of interest for application purposes in climate models and, in particular, in GCM-type models in which computational speed is a critical parameter. The suggested numerical scheme achieves the same computational efficiency as Sasamori's simplified scheme, even though it goes through the double integrations.

For the purpose of comparing the results, $\langle T\rangle_A$ of the modified scheme was calculated from the new values of $F^{\uparrow}$ by solving (2) for $\langle T\rangle_A$. The comparison is shown in Table 1, demonstrating that the first term on the right-hand side of (4) is the largest source of difference (~0.4 W m^{-2} °C^{-1}). Values of $(\partial F^{\uparrow}/\partial T_s)_{r,\gamma}$ obtained with Sasamori's method are high compared to estimates mentioned in the Introduction (section 1).

Checking the value of $(\partial\langle T\rangle_A/\partial T_s)_{r,\gamma}$ has shown that it ≃1.0 in Sasamori's simplified method while it =0.7 in the modified scheme. It is therefore apparent that the use of the "mean source function" in Sasamori's treatment has kept the effective emission of the atmosphere at a constant height. A rise in T_s while holding γ constant has resulted in an equal rise in $\langle T\rangle_A$.

In the modified scheme, on the other hand, the increase in the water vapor content of the atmosphere associated with the rise in T_s has caused a rise in the atmospheric absorptivity (emissivity), implying a higher altitude for the effective emitting temperature of the atmosphere, and resulting in a value of $(\partial\langle T\rangle_A/\partial T_s)_{r,\gamma}$ which is lower than unity.

The terms involving $\partial\bar{A}_0/\partial T_s$ derivatives have contributed little to the difference in $(\partial F^{\uparrow}/\partial T_s)_{r,\gamma}$ between the two schemes. This result is to be expected since the broadband water vapor emissivity is relatively insensitive to temperature. (The flux emissivity is inversely proportional to the temperature in the H_2O rotation region but directly proportional to temperature in the window and vibration–rotation regions.)

3. The cloud-top variation mechanism

For standard conditions, $T_s = 288$ K, $\gamma = 6.5$°C km^{-1}, $r = 0.75$, $A_c = 0.5$ (and also $q = q_s(p/p_s)^{\lambda}$ with $\lambda = 3.0$ and $z_t = 13$ km), the new longwave scheme yields $F^{\uparrow}_{\text{clear}} = 253$ W m^{-2} and $F^{\uparrow}_{\text{cloud}} = 192$ W m^{-2} (with a hemispherically averaged effective cloud-top altitude, $\bar{z}_c$, of 5.5 km), which is written here for convenience as $F^{\uparrow} = 253 - 61A_c = 222$ (with $A_c = 0.5$).[2] Perturbing T_s by $\Delta T_s = +1$°C while holding γ, r and A_c constant and fixing the cloud-top altitude (FCA) results in

$$\left(\frac{\partial F^{\uparrow}}{\partial T_s}\right)_{r,\gamma,A_c} = 2.22 + 0.33A_c = 2.39 \quad [\text{W m}^{-2}\ ^{\circ}\text{C}^{-1}]. \tag{5}$$

This result is compared with the results of two other radiative transfer models employing globally averaged conditions—the FCA model of Cess (1974)

$$F^{\uparrow} = 256 - 71A_c = 220 \qquad [\text{W m}^{-2}] \tag{6}$$

$$\left(\frac{\partial F^{\uparrow}}{\partial T_s}\right)_{r,\gamma,A_c} = 1.95 + 0.42A_c = 2.16 \quad [\text{W m}^{-2}\ ^{\circ}\text{C}^{-1}] \tag{7}$$

and the FCA model of Ramanathan et al. (1976)

$$F^{\uparrow} = 258 - 71A_c = 226^{3} \qquad [\text{W m}^{-2}] \tag{8}$$

$$\left(\frac{\partial F^{\uparrow}}{\partial T_s}\right)_{r,\gamma,A_c} = 2.16 + 0.185A_c = 2.25^{3} \quad [\text{W m}^{-2}\ ^{\circ}\text{C}^{-1}]. \tag{9}$$

Cess (1974) and Ramanathan et al. (1976) have compared their results to those of the semiempirical study of Budyko (1969), who has used the results of calculations of monthly mean values of $F^{\uparrow}$ from 260 stations (calculated from vertical profiles of T_s, r and γ, see Cess, 1976) to find a regression formula of the form

$$F^{\uparrow} = 233 + 2.2T_s - (4.7 + 1.6T_s)A_c, \tag{10}$$

where the units of $F^{\uparrow}$ and T_s are W m^{-2} and °C, respectively. Equation (10) yields (with $T_s = 15$°C)

$$F^{\uparrow} = 256 - 71A_c = 220 \qquad [\text{W m}^{-2}] \tag{11}$$

$$\left(\frac{\partial F^{\uparrow}}{\partial T_s}\right)_{A_c} = 2.23 - 1.6A_c = 1.43 \quad [\text{W m}^{-2}\ ^{\circ}\text{C}^{-1}]. \tag{12}$$

[2] This implies that $\partial F^{\uparrow}/\partial A_c = 61$ W m^{-2}. Raising $\bar{z}_c$ from 5.5 km to 6.3 km results in $\partial F^{\uparrow}/\partial A_c = 70$ W m^{-2}. See discussion on the method of calculation of z_c.

[3] With $A_c = 0.5$.

Comparison of Eq. (12) with Eqs. (5), (7) and (9) shows substantially lower $\delta F^{\uparrow}/\delta T_s$ values over clouds in Budyko's results, in complete disagreement with the FCA models of Cess, Ramanathan et al. and with the present study. [Note, however, that the definition of $\delta F^{\uparrow}/\delta T_s$ is different in (12).]

Both Cess and Ramanathan et al. have therefore suggested a fixed cloud-top *temperature* (FCT) model, recommending its use for the modeling of climate change. With FCT, Cess obtained

$$\left(\frac{\partial F^{\uparrow}}{\partial T_s}\right)_{r,\gamma,A_c} = 1.95 - 1.74A_c = 1.08 \quad [\mathrm{W\ m^{-2}\ ^{\circ}C^{-1}}]\ \mathrm{FCT}, \tag{13}$$

and Ramanathan et al. obtained

$$\left(\frac{\partial F^{\uparrow}}{\partial T_s}\right)_{r,\gamma,A_c} = 2.16 - 1.75A_c = 1.28^{4} \quad [\mathrm{W\ m^{-2}\ ^{\circ}C^{-1}}]\ \mathrm{FCT}. \tag{14}$$

With FCT, the present longwave scheme yields

$$\left(\frac{\partial F^{\uparrow}}{\partial T_s}\right)_{r,\gamma,A_c} = 2.22 - 1.73A_c = 1.35 \quad [\mathrm{W\ m^{-2}\ ^{\circ}C^{-1}}]\ \mathrm{FCT}. \tag{15}$$

An examination of the *total* $\delta F^{\uparrow}/\delta T_s$ values in Eqs. (13–15) reveals that these values are rather low in comparison with estimates of $\delta F^{\uparrow}/\delta T_s$ mentioned in the Introduction (section 1), although the variations in the definition of the longwave sensitivity parameter and the fact that different sampling techniques are used may certainly affect the results.

Cess (1976) has performed an observational study, using annual mean satellite data of $F^{\uparrow}$ of Ellis and Vonder Haar (1976). A Budyko-type correlation with annual data of T_s and A_c has yielded

$$\left(\frac{\partial F^{\uparrow}}{\partial T_s}\right)_{A_c} = 1.6 - 0.07A_c = 1.57 \quad [\mathrm{W\ m^{-2}\ ^{\circ}C^{-1}}]. \tag{16}$$

Equation (16) seemed to change the previous conclusion of Cess (1974) and Ramanathan et al. (1976) with regard to the FCT model.

More recent observational studies have not settled the question of which of the two models, the FCA and the FCT, was more accurate. Table 2 summarizes the study of Simmonds and Chidzey (1982), in which different regression experiments were performed on two datasets of satellite measurements of $F^{\uparrow}$, using a Budyko-type correlation of the form

$$F^{\uparrow} = a + bT_s + cA_c + dT_s \cdot A_c. \tag{17}$$

[4] With $A_c = 0.5$.

TABLE 2. Comparison of values for $(\partial F^{\uparrow}/\partial T_s)_{A_c} = b + dA_c$ obtained from different experiments and satellite data (after Simmonds and Chidzey, 1982).

Experiment					
Hemisphere	Period	Data	b	d	$(\partial F^{\uparrow}/\partial T_s)_{A_c}$
NH	Annual	EV	1.70	−0.12	1.64
NH	Annual	W	2.96	−3.24	1.34
SH	Annual	EV	1.68	−0.13	1.62
SH	Annual	W	1.60	−0.11	1.55
Global	Annual	EV	1.03	+1.16	1.61
Global	Annual	W	1.98	−0.99	1.49
NH	Seasonal	EV	2.55	−1.68	1.71
NH	Seasonal	W	2.42	−1.89	1.48
SH	Seasonal	EV	2.86	−2.39	1.67
SH	Seasonal	W	1.85	−0.52	1.59
Global	Seasonal	EV	2.45	−1.58	1.66
Global	Seasonal	W	2.06	−1.03	1.55

Taking the T_s partial derivative, holding A_c constant, gives

$$\left(\frac{\partial F^{\uparrow}}{\partial T_s}\right)_{A_c} = b + dA_c. \tag{18}$$

In the annual experiment, Simmonds and Chidzey applied the regression Eq. (17) at every 10° of latitude for hemispheric and global experiments. In the seasonal experiments, 9 × 4 and 18 × 4 sets of values, respectively, were used at every 10° of latitude and for 3 months. In Table 2, EV refers to the dataset of Ellis and Vonder Haar (1976) and W refers to the dataset of Winston et al. (1979).

Table 3 shows the results of a regression analysis of the form of Eq. (17) performed for 2 months of daily global (500 km grid) data (Ohring and Chen, 1986, personal communication). The $F^{\uparrow}$ values are from NIMBUS-7 NFOV ERB and the T_s values are from USAF data.

The observational results of Tables 2 and 3, therefore, do show some support for the FCT model, since d is generally negative. However, the magnitude of the observed values of d varies between that predicted by the FCT and FCA models. Thus, it seems that the correct approach to settling the question of FCT vs FCA is not a Budyko-type correlation of the form (17), but a direct observational correlation between the cloud-top temperature T_c and the surface temperature T_s, of the form:

$$T_c = A + BT_s. \tag{19}$$

Ohring and Adler (1978) have determined the average height of the cloud top $z_c(\phi)$ for a single effective cloud at each latitude ϕ by weighting the cloud-top heights in the three-layer model of Manabe (1969) (which is based upon the climatological analysis of cloud statistics by London, 1957) by the amount of each cloud type visible from space. Figure 1 shows the

TABLE 3. Comparison of values for $(\partial F^{\uparrow}/\partial T_s)_{A_c} = b + dA_c$ obtained by correlating 2 months of daily global observations (500 km grid).

Experiment	b	d	$(\partial F^{\uparrow}/\partial T_s)_{A_c}$
Jan. 1980	2.40	−1.75	1.52
July 1979	2.42	−1.32	1.76

dependence of $z_c(\phi)$ on latitude (top) and on the mean-annual observed $T_s(\phi)$ (bottom) from Oort and Rasmusson (1971). In the present study, these values of $z_c(\phi)$ were used to calculate $T_c(\phi)$ (the cloud-top temperature at each latitude ϕ) by interpolation from the mean-annual data of geopotential height and temperature of Oort and Rasmusson (1971). Using the resulting values of T_c and the mean-annual 1000-mb temperatures of Oort and Rasmusson for T_s has resulted in

$$T_c = -20.3 + 0.45T_s \qquad (20)$$

with a correlation coefficient of $r = 0.998$. These results are plotted in Fig. 2. Equation (20) implies that $dT_c/dT_s = 0.45$. Note that with FCT, T_c does not change with T_s variations, i.e., $dT_c/dT_s = 0$; and that FCA implies equal changes in T_c and T_s, provided γ is constant, i.e., $dT_c/dT_s = 1$.

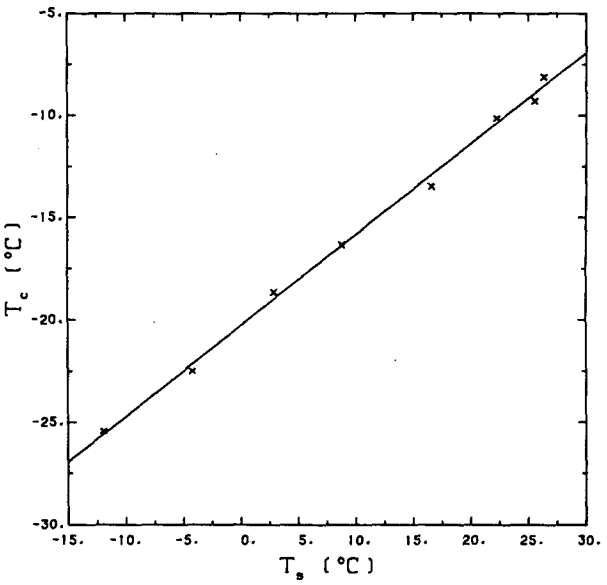

FIG. 2. Correlation between the cloud-top temperature $T_c(\phi)$ (for a single effective cloud layer, see text) and the surface temperature $T_s(\phi)$.

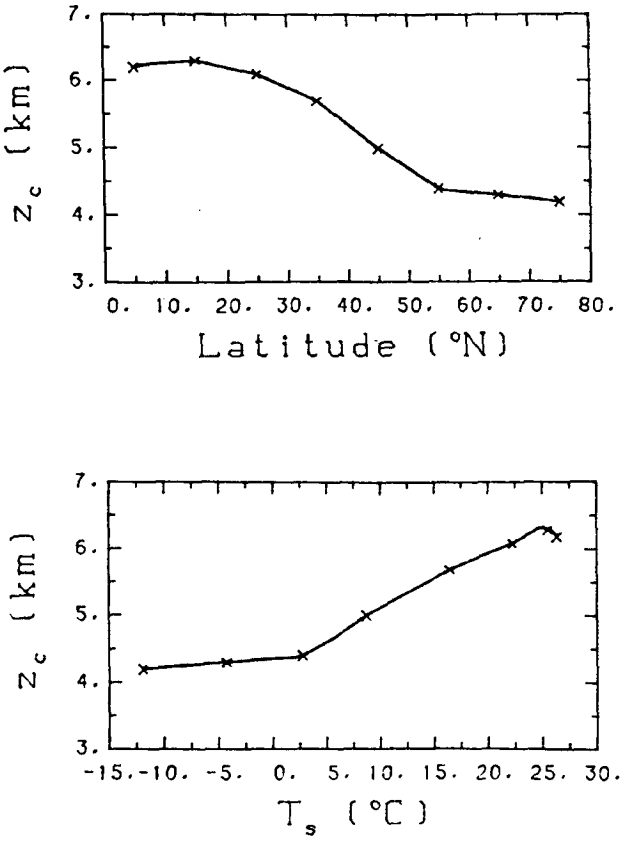

FIG. 1. The dependence of the cloud-top height $z_c(\phi)$ on latitude (top) and on the surface temperature $T_s(\phi)$ (bottom), for a single effective cloud layer (see text).

Therefore, this result strengthens the impression obtained above from the Budyko-type correlations, that the observed longwave sensitivity parameter lies between the predicted values of the FCA and FCT models. It is stressed that Eq. (20) was derived from zonal and annually averaged conditions. The actual value of the coefficient B may vary in time and, of course, the correlation does not necessarily hold regionally. It is suggested that correlations of the type (19) be performed on time-dependent data of T_c and T_s, should these data be available.

Based on the above discussion, a *variable cloud-top temperature* (VCT) model is presently suggested. Let $z_{c0}(\phi)$, $T_{c0}(\phi)$, $T_{s0}(\phi)$ and $\gamma_0(\phi)$ denote the cloud-top height, cloud-top temperature, surface temperature and lapse rate, respectively, for *mean-annual conditions,* as computed and discussed before. The actual cloud-top temperature $T_c(\phi)$ is written as

$$T_c(\phi) = T_{c0}(\phi) + \alpha[T_s(\phi) - \gamma(\phi) \times (z_{c0}(\phi) - z_s(\phi)) - T_{c0}(\phi)] \qquad (21)$$

where $T_s(\phi)$ and $\gamma(\phi)$ are the actual surface temperature and lapse rate, respectively, and $z_s(\phi)$ is the surface elevation. With $\alpha = 0$, $T_c(\phi) = T_{c0}(\phi)$, giving the FCT model. With $\alpha = 1$, Eq. (21) reduces to $T_c(\phi) = T_s(\phi) + \gamma(\phi) \cdot z_{c0}(\phi)$, giving the FCA model. For the suggested VCT model, $\alpha = 0.45$, in agreement with the requirement that $dT_c/dT_s = 0.45$. Equation (21) satisfies the

mean-annual conditions, i.e., substituting $T_s(\phi) = T_{s0}(\phi)$ and $\gamma(\phi) = \gamma_0(\phi)$ into Eq. (21) gives $T_c(\phi) = T_{c0}(\phi)$.

The experiment described at the beginning of this section, for standard conditions, was performed again with the VCT formulation, yielding

$$\left(\frac{\partial F^{\uparrow}}{\partial T_s}\right)_{r,\gamma,A_c} = 2.22 - 0.80A_c = 1.82 \text{ [W m}^{-2}\text{ °C}^{-1}\text{] VCT,} \quad (22)$$

which indeed shows better agreement with observations.

The discussion up to this point has been limited to a comparison of the performance of the longwave scheme models under standard conditions defined at the beginning of this section. In section 4, the longwave scheme is implemented into a climate model and the results of its performance with the VCT and FCA models is compared.

4. Results with a climate model

The climate model utilized for the verification of the longwave scheme and the evaluation of the differences between the VCT and FCA models is a version of the hemispheric dynamic zonally averaged model of OA. A full description of this version can be found in Neeman (1986a). Following is a short summary of the structure of the climate model.

The model is based upon the zonally averaged form of the two-level, quasi-geostrophic potential vorticity system of equations, including diabatic heating and frictional dissipation. The quasi-geostrophic eddy transport is parameterized according to a relation between the eddy exchange coefficients and the meridional temperature gradient in the atmosphere (Neeman et al., 1986c). At the surface level, a heat budget equation is applied separately to an oceanic portion and to "glacier" and "nonglacier" continental portions for Eurasia and North America. Each land type has different heat storage characteristics and has a specified topography and fraction at each latitude belt. Sea ice/snow and land snow are modeled using a vertically integrated formulation that has the capability of simulating the nonlinear effects of heat transfer through the layers of ice and snow (Neeman et al., 1986b). The atmospheric heating term is the weighted average of the contributions from each land type according to its fraction and is used to calculate the zonally averaged temperature at 500 mb. Surface and atmospheric heating processes included are solar radiation (absorption by water vapor, ozone and cloud particles), longwave radiation (as described before), convection, evaporation at the surface, condensation in the atmosphere, subsurface heating and ocean currents.

Two climate model runs are examined subsequently. The two runs are identical except for the parameter α of the cloud-top variation mechanism (section 3), which is varied between 0.45 (the VCT model) and 1.0 (the FCA model). As an observational verification, use is made of the zonal (10° lat) means of radiation budget data from the two-channel scanning radiometer aboard the NOAA operational polar-orbiting satellites, in the period between June 1974 and March 1978 (Gruber and Krueger, 1984). These data are hereafter referred to as NOAA SR.

The latitudinal dependence of the annually averaged longwave flux emitted at the top of the atmosphere is shown in Fig. 3 for the VCT and FCA climate model runs and for the annually averaged NOAA SR data. Only a slight difference of less than ~ 2 W m^{-2} can be detected between the VCT and FCA runs, and there is a fairly good agreement between both runs and the NOAA SR data. (The lack of difference between the annually averaged results of the VCT and FCA models is further discussed later.)

Figure 4 shows the seasonal cycle of the hemispherical average (excluding latitude belts 5° and 15°N) of the longwave radiation for the two runs and NOAA SR. The two tropical latitude belts were excluded in this average in order not to take into account inaccuracies in the simulation of longwave radiation in the tropics, connected with the excess of ~ 2°C predicted for T_s at these latitudes. The latter is a consequence of the lack of explicit treatment of the Hadley circulation and the seasonal movement of the ITCZ, with its related changes in the cloud distribution, and also of the absence of heat transport across the equator (see discussion in Neeman, 1986a). Whereas there was little

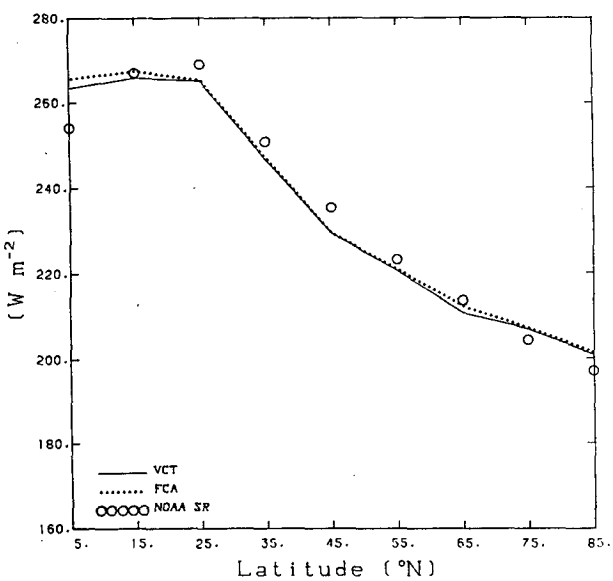

FIG. 3. The latitudinal dependence of the annually averaged longwave flux emitted at the top of the atmosphere, for the VCT and FCA climate model runs and for the annually averaged NOAA SR observational data (see text).

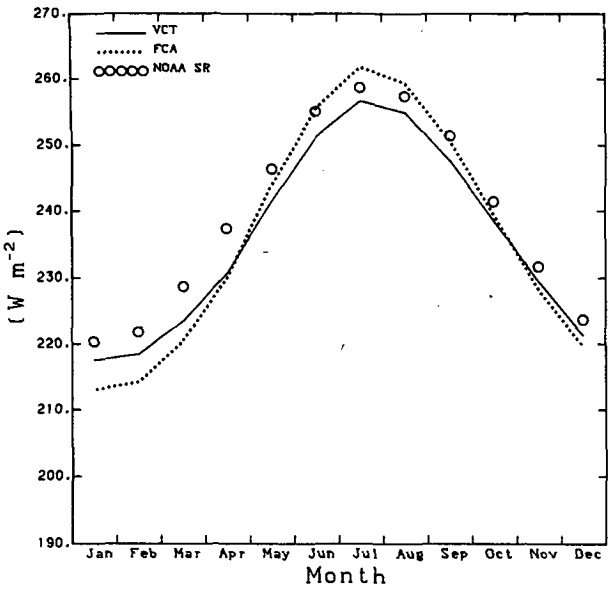

FIG. 4. The seasonal cycle of the hemispherical average (excluding latitude belts 5° and 15°N) of the longwave radiation at the top of the atmosphere, for the VCT and FCA climate model runs and for the annually averaged NOAA SR observational data (see text).

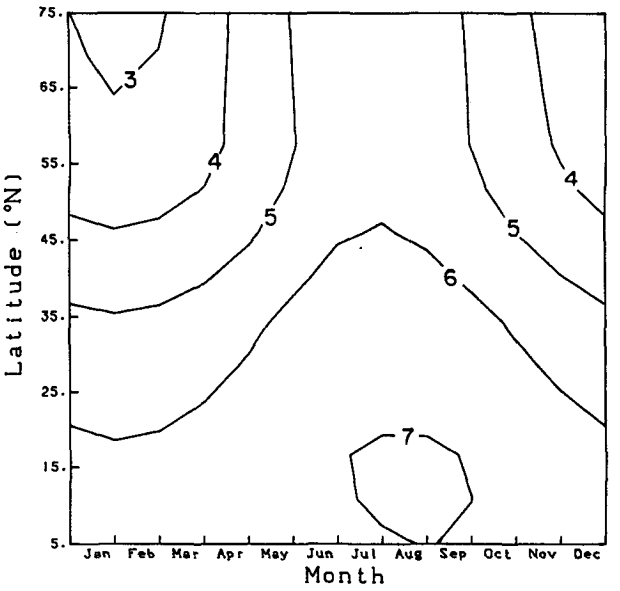

FIG. 5. The latitude–time cross section of the effective cloud-top elevation, as simulated by the VCT (variable cloud-top temperature) model run.

difference between these two runs in the simulated annually averaged flux, the FCA run fails to reproduce the correct amplitude of seasonal variation in the outgoing terrestrial radiation by overestimating this amplitude by as much as 25%. The reason for this behavior is the higher sensitivity of the outgoing longwave radiation to changes in the surface temperature ($\delta F^{\uparrow}/\delta T_s$) in the FCA run. In the VCT run, the cloud-top variation mechanism lowers the resulting $\delta F^{\uparrow}/\delta T_s$ and thus reproduces a smaller seasonal change in $F^{\uparrow}$, in agreement with the observations (within 5%).

The cloud-top elevation as a function of latitude and time of year, as simulated by the VCT mechanism, is plotted in Fig. 5. In the FCA run, the cloud-top elevation does not change in time, and can be seen in Fig. 1.

The differences in the simulated amplitudes of the outgoing longwave radiation amount to ~ 10 W m^{-2} between the VCT and FCA runs. This difference is too small to significantly affect the seasonal cycle of the overall heat balance, due to the domination of the subsurface heat storage lag effect, which results in differences of no more than ~ 1°C in the seasonal surface temperature amplitude between the two runs (Fig. 6). The feedback between $F^{\uparrow}$ and the surface temperature manifests itself more strongly in long-term climate changes, which unlike the seasonal cycle, reach a state of equilibrium. This will now be demonstrated for changes in the solar constant.

a. Sensitivity to the solar constant

In this experiment, each of the VCT and FCA climate model runs were rerun, each time starting from the same initial conditions and proceeding until equilibrium, with the solar constant value changed by ±1%. Table 4 lists the values of β_0^-/β_0^+ for the VCT and FCA runs, defined as the decrease/increase in the annually hemispherically averaged surface temperature followed by lowering/raising the present solar constant by 1%. The sensitivity of the VCT run is therefore shown to be about twice as large as that of the FCA run.

Note that the values of β_0^- are about three times larger than those of β_0^+. This nonlinearity is a consequence of the nonlinear character of the climate system: For example, as the solar constant decreases from +1% to −1% of its present value, the global temperature is lowered and larger continental fractions are involved

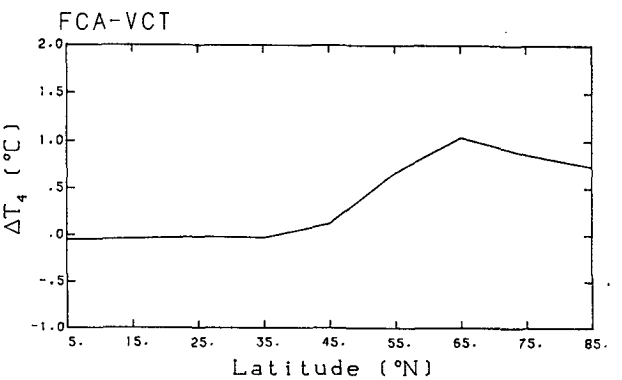

FIG. 6. The difference [FCA minus VCT] in the amplitude of the seasonal cycle of zonally averaged surface temperature (T_4, in °C) simulated by the two climate model runs.

TABLE 4. The sensitivities β_0^- and β_0^+ for the VCT and FCA model runs (in °C).

Model	β_0^-	β_0^+
VCT	1.8	0.6
FCA	1.0	0.3

in the snow albedo–temperature *positive* feedback, leading to increasing sensitivity with decreasing solar constant. (See Neeman et al., 1986d, for a more detailed discussion.)

The annually averaged *difference* in the zonally averaged surface temperature, ΔT_4, between the -1% experiment and the standard run for each of the VCT and FCA runs, as a function of latitude, is shown in Fig. 7. Figure 8 is a repeat of the last figure for the 500-mb temperature, T_2. The difference in the response of the VCT and FCA model runs resulting from a decrease of 1% in the solar constant are therefore larger at high latitudes, and they peak at the surface at latitude belt 55°N, where the sensitivity of the VCT model is three times larger than the FCA.

These results agree with the conclusions of Warren and Schneider (1979) and Hartmann and Short (1979), where $B = dF^{\uparrow}/dT_s$ (for a parameterization of the type of $F^{\uparrow} = A + BT_s$) has been varied arbitrarily in the range of its uncertainty and the climate sensitivity examined. (See also detailed discussion in Neeman, 1986a.)

5. Conclusions

This study describes a modified radiation scheme that simulates the water vapor–temperature (opacity) feedback mechanism and that has a provision for a *variable cloud-top temperature* (VCT) model. The modified scheme has been shown to decrease the clear sky sensitivity of the outgoing longwave radiation to changes in the surface temperature to a value of 2.2 W m^{-2} °C^{-1}, compared to the original high value of 2.6 W m^{-2} °C^{-1} in a scheme based on a simplified method suggested originally by Sasamori (1970) and used in a variety of climate models in order to reduce time consumption. The physical reason for the opacity feedback is that as the temperature of the atmosphere rises, its ability to hold water vapor also rises, increasing its opacity and effective level of emission and decreasing its ability to radiate to space. In Sasamori's simplification the effective level of emission remains essentially constant with a change in surface temperature, leading to an underestimate of the opacity feedback. The modified scheme has the same computational efficiency as that of the original simplified scheme of Sasamori (1970), and is therefore ideally suited for implementation in large GCM-type models.

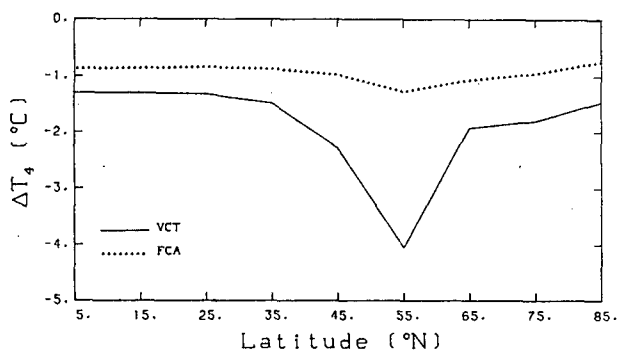

FIG. 7. The latitudinal dependence of the annually averaged differences in T_4 [-1% experiment minus standard run], for each of the VCT and FCA climate model runs.

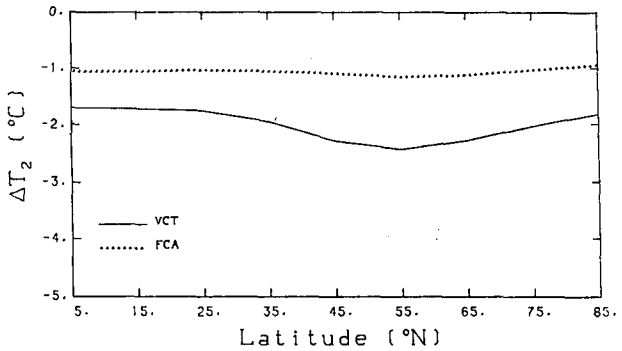

FIG. 8. As in Fig. 7, but for the 500-mb temperature, T_2.

However, over the cloud portion of the sky, the value of $\partial F^{\uparrow}/\partial T_s$ has remained high (2.55 W m^{-2} °C^{-1}), since the column of air that participates in the water vapor–temperature feedback is smaller (i.e., only above the cloud top). The higher value of $\partial F^{\uparrow}/\partial T_s$ over the cloud portion of the sky is common to all models that use a fixed cloud-top altitude (FCA), and has motivated the introduction of the fixed cloud-top temperature (FCT) model (Cess, 1974; Ramanathan et al., 1976).

Observational studies analyzing the Budyko-type correlation of the form $F^{\uparrow} = a + bT_s + cA_c + dT_s \cdot A_c$ have not settled the question of FCA vs FCT, since they show values of d that vary between those predicted by the FCA and FCT models. The approach suggested by the present study is to apply a direct observational correlation between the effective cloud-top temperature T_c and the surface temperature T_s, of the form $T_c = A + BT_s$. A regression analysis based on annually averaged cloud statistics data has yielded $B = 0.45$ with a high correlation coefficient. It is suggested that correlations of this type be performed on time-dependent data of T_c and T_s, should these data be available.

Consequently, a *variable cloud-top temperature* (VCT) model has been suggested in this study, with a tunable parameter α. With $\alpha = 1$, or $\alpha = 0$, the model

reduces to the FCA or FCT, respectively; and with an intermediate $\alpha = 0.45$, the VCT meets the preceding observational result, resulting in $\partial F^{\uparrow}/\partial T_s = 1.82$ W m^{-2} °C^{-1} over the combined cloud/clear sky.

The implementation of the longwave scheme into a zonally averaged dynamic climate model has demonstrated that the suggested VCT model with $\alpha = 0.45$ almost doubles the sensitivity of the climate model to solar constant changes ($\beta_0^- = 1.8$°C), compared to the FCA model ($\beta_0^- = 1.0$°C). On the other hand, the VCT and FCA models were quite similar in their simulation of the present climate, stressing that an agreement with current observed fields does not automatically guarantee a correct performance in climate change experiments. These results emphasize the importance of simulating the correct longwave *sensitivity* to temperature changes, and not only the correct longwave flux, by radiation schemes employed in climate models which investigate climate change. The conclusions of the present study are applicable to the higher-level climate models and emphasize the importance of more sophisticated cloud modeling in future study. In particular, these conclusions indicate that GCMs in which the cloud tops are not allowed to change in height suffer from a reduced sensitivity by a factor approaching 2.

Acknowledgments. This study was carried out as part of the requirements for the Ph.D. degree of the first author at Tel-Aviv University.

APPENDIX A

The Modified Longwave Scheme

The basic equations are the "radiation chart" radiative transfer equations without making use of the Sasamori's (1970) simplification. In fact, they are similar to those of Sasamori (1968) with the exception that the absorptivity $\bar{A}(u, T)$ is not approximated by $\bar{A}_0$ except where mentioned subsequently. [This assumption is hereafter referred to as the $\bar{A}_0(u)$ approximation]

$$F^{\uparrow}_{\text{clear}} = \sigma T^4(z_s) + 4\sigma \int_{T(z_s)}^{T(z_t)} \bar{A}[u(T') - u(0), T']T'^3 dT' \quad \text{(A1.1)}$$

$$F^{\uparrow}_{\text{cloud}} = \sigma T^4(z_c) + 4\sigma \int_{T(z_c)}^{T(z_t)} \bar{A}[u(T') - u(0), T']T'^3 dT' \quad \text{(A1.2)}$$

$$F^{\downarrow}_{\text{clear}} = -4\sigma \int_{T(z_s)}^{T(z_t)} \bar{A}\{u(T') - u[T(z_s)], T'\}T'^3 dT' + \sigma T^4(z_t) \cdot \bar{A}\{u[T(z_t)] - u[T(z_s)], T(z_t)\} \quad \text{(A1.3)}$$

$$F^{\downarrow}_{\text{cloud}} = \sigma T^4(z_b) - 4\sigma \int_{T(z_s)}^{T(z_b)} \bar{A}\{u(T') - u[T(z_s)], T'\}T'^3 dT' \quad \text{(A1.4)}$$

where $F^{\uparrow}$ is the upward flux at the top of the atmosphere, $F^{\downarrow}$ is the downward flux at the bottom of the atmosphere, z_s, z_b, z_c and z_t are the surface elevation, cloud base elevation, cloud top elevation (for a single effective cloud layer, see subsequent discussion) and tropopause elevation, respectively; and where $\bar{A}(u, T)$ is as evaluated by Sasamori (1968) making use of

$$4\sigma \int_{T(z_t)}^{0} \bar{A}\{u(T') - u[T(z_s)], T'\}T'^3 dT' = \sigma T^4(z_t) \cdot \bar{A}\{u[T(z_t)] - u[T(z_s)], T(z_t)\} \quad \text{(A1.5)}$$

where it has been assumed that above z_t, the pathlength changes very little.

A potential problem in using the set of Eqs. (5)–(8) without Sasamori's simplification and without the $\bar{A}_0$ approximation is an excessive computing time consumption due to repeated calculation of $\bar{A}(u, T)$ and $u(T)$ inside the vertical integrals. Sasamori (1968) has used a cubic interpolation formula in terms of u and T to read $R(u, T)$ from the Atmospheric Radiation Tables (ART) of Elsasser and Culbertson (1960), and since the change in $R(u, T)$ for small values of u is large, supplemental grid points had to be inserted to the original points. To reduce computing time, Sasamori has therefore suggested the $\bar{A}_0$ approximation,

TABLE A1. The value of $\bar{A}(u, T)$ for water vapor, as a function of the effective pathlength u (gm) and the temperature T (°C), calculated from $R(u, T)$ of Table 18 of ART (see text).

	Temperature (°C)												
$\log_{10}u$	−80	−70	−60	−50	−40	−30	−20	−10	0	10	20	30	40
−5	0.013	0.014	0.014	0.014	0.014	0.015	0.016	0.017	0.018	0.020	0.021	0.022	0.023
−4	0.043	0.042	0.041	0.042	0.042	0.043	0.044	0.045	0.047	0.049	0.051	0.053	0.055
−3	0.111	0.107	0.105	0.104	0.104	0.105	0.106	0.108	0.111	0.114	0.117	0.121	0.124
−2	0.212	0.205	0.201	0.199	0.199	0.201	0.205	0.209	0.214	0.220	0.226	0.233	0.239
−1	0.325	0.318	0.314	0.313	0.314	0.318	0.324	0.331	0.340	0.349	0.359	0.369	0.380
0	0.475	0.472	0.472	0.475	0.480	0.487	0.496	0.506	0.517	0.530	0.542	0.556	0.570
1	0.721	0.731	0.743	0.756	0.770	0.785	0.800	0.816	0.831	0.846	0.861	0.876	0.890

TABLE A2. The correction array for the temperature dependence of $\bar{A}(u, T)$ for water vapor, as a function of the effective pathlength u (gm) and the temperature T (°C).

	Temperature (°C)												
$\log_{10}u$	−80	−70	−60	−50	−40	−30	−20	−10	0	10	20	30	40
−5	−0.004	−0.003	−0.003	−0.003	−0.003	−0.002	−0.001	0.000	0.001	0.003	0.004	0.005	0.006
−4	−0.003	−0.004	−0.005	−0.004	−0.004	−0.003	−0.002	−0.001	0.001	0.003	0.005	0.007	0.009
−3	0.001	−0.003	−0.005	−0.006	−0.006	−0.005	−0.004	−0.002	0.001	0.004	0.007	0.011	0.014
−2	0.000	−0.007	−0.011	−0.013	−0.013	−0.011	−0.007	−0.003	0.002	0.008	0.014	0.021	0.027
−1	−0.010	−0.017	−0.021	−0.022	−0.021	−0.017	−0.011	−0.004	0.005	0.014	0.024	0.034	0.045
0	−0.035	−0.038	−0.038	−0.035	−0.030	−0.023	−0.014	−0.004	0.007	0.020	0.032	0.046	0.060
1	−0.095	−0.085	−0.073	−0.060	−0.046	−0.031	−0.016	0.000	0.015	0.030	0.045	0.060	0.074

and has fitted empirical formulas for $\bar{A}_0(u)$ from Yamamoto's (1952) chart.

In the present study, the temperature dependence of $\bar{A}(u, T)$ for water vapor is considered to have possible important implications and is therefore not neglected. Sasamori's original approach of using the ART is modified and implemented. (The ART has a larger temperature dependence for $\bar{A}(u, T)$ for water vapor than Yamamoto's chart; see Fig. 4 of Sasamori, 1968.) The technical problems mentioned in the former paragraph were overcome by employing the Sasamori $\bar{A}_0(u)$ formula for water vapor as a reference and using a correction array for the temperature dependence of $\bar{A}(u, T) = R(u, T)/4\sigma T^3$, where $R(u, T)$ is given (in cal cm^{-2} day^{-1}) in Table 18 of the ART. The variable $\bar{A}(u, T)$ and the correction array are tabulated in Tables A1 and A2, respectively. Since the correction values are small in magnitude, it is possible to use a simple bilinear interpolation without seriously affecting time consumption.

The reference formula for $\bar{A}_0$ for water vapor is slightly modified in the present study:

$$\bar{A}_0(u) = \begin{cases} 0.846(u + 3.59 \cdot 10^{-5})^{0.243} - 6.229 \cdot 10^{-2}, \\ \qquad\qquad u < 0.01 \text{ gm} \\ 0.240 \log_{10}(u + 0.01) + 0.622, \\ \qquad\qquad 0.01 \leq u < 5 \text{ gm}. \end{cases} \tag{A1.6}$$

The original formula, Eqs. (14) and (15) of Sasamori (1968), has a discontinuity at $u = 0.01$ gm, while the above formula does not. The $\bar{A}_0$ approximation of Sasamori is retained in the present study for the carbon dioxide absorptivity and for the correction of the 15 μm band overlap of carbon dioxide and water vapor absorption, due to their smaller effect.

In order to overcome the problem of repeated use of logarithmic and power functions inside the vertical integrals, the effective pathlength of water vapor and carbon dioxide are transformed into power functions of a single variable T/T_s (appendix B).

In order to perform the vertical integration, the troposphere is divided into three unequal large temperature intervals partitioned by the boundaries of the effective cloud layer: $\Delta T_1 = T(z_s) - T(z_b)$, $\Delta T_2 = T(z_b) - T(z_c)$ and $\Delta T_3 = T(z_c) - T(z_t)$. For a model with n cloud layers, this procedure is generalized by dividing the troposphere into $2n + 1$ large unequal temperature intervals, ΔT_i, partitioned by n cloud layers. Each interval ΔT_i is further subdivided into m_i equal smaller intervals, such that m_i is the integer value of $|\Delta T_i/\gamma \Delta z|$, where γ is the lapse rate and Δz is the desired vertical resolution. The $\bar{A}(u, T)$ and T^3 are calculated at the middle of each subinterval (the midpoint rule). This has been found to be less time consuming than other integration rules and sufficiently accurate.

An estimate of the accuracy of the numerical scheme is shown in Table A3. As the vertical resolution increases, the solution converges. Therefore, the $\Delta z = 10$ m solution is taken as a reference. These results show that the numerical scheme presented here is sufficiently accurate (a relative error of less than 1%) for standard climate modeling purposes, with a vertical resolution of ~1 km. With this vertical resolution, the modified longwave scheme has completely overcome the problems of computer time consumption, achieving the same efficiency as that of the Sasamori (1970) simplified scheme.

TABLE A3. Estimate of the accuracy of the numerical scheme, with reference to a vertical resolution of 0.01 km.

vertical resolution (m)	Relative error $(\partial F^{\uparrow}/\partial T_s)_{r,\gamma}$ (%)	Absolute error $(\partial F^{\uparrow}/\partial T_s)_{r,\gamma}$ (W m^{-2} °C^{-1})	Absolute error $F^{\uparrow}$ (W m^{-2})
10	0	0	0
100	<0.4	<0.01	<1.
1000	0.4	0.01	<1.
3000	1.3	0.03	1.

APPENDIX B

The Transformed Effective Pathlengths

The effective path length is given by (e.g., OA)

$$u[p_2,p_1]=\frac{1}{g}\int_{p_1}^{p_2} q\frac{p}{p_0}\left(\frac{T}{T_0}\right)^{-1/2}dp$$
$$=\frac{c_0}{g}\int_{p_1}^{p_2} q\frac{p}{p_s}\left(\frac{T}{T_s}\right)^{-1/2}dp \qquad \text{(A2.1)}$$

where p_1 and p_2 are the pressures at the top and bottom of the air column, respectively; g is the gravity constant; q the mixing ratio of the absorbing gas; p_0 and T_0 are the STP values of pressure and temperature, respectively; the s subscript denotes surface values; and

$$c_0=\frac{p_s}{p_0}\left(\frac{T_0}{T_s}\right)^{-1/2}.$$

In the troposphere, a constant lapse rate γ is assumed, and therefore

$$\frac{dp}{p}=-\frac{g}{RT}dz=\frac{g}{RT\gamma}dT. \qquad \text{(A2.2)}$$

Integration of (A2.2) from $p_s(T_s)$ to $p(T)$ gives the standard formula for a constant lapse-rate atmosphere

$$\frac{p}{p_s}=\left(\frac{T}{T_s}\right)^{\Gamma/\gamma} \qquad \text{(A2.3)}$$

where $\Gamma = g/R$ and R is the gas constant for dry air. Rearranging (A2.1) and substituting (A2.2) and (A2.3) gives

$$u[p_2(T_2),p_1(T_1)]=\frac{c_0p_s}{g}\int_{p_1}^{p_2} q\left(\frac{p}{p_s}\right)^2\left(\frac{T}{T_s}\right)^{-1/2}\frac{dp}{p}$$
$$=\frac{c_0p_s}{R\gamma}\int_{T_1}^{T_2} q\left(\frac{T}{T_s}\right)^{[2\Gamma/\gamma-1/2]}\frac{dT}{T}$$
$$=\frac{c_0p_s}{R\gamma}\frac{1}{T_s^{[2\Gamma/\gamma-1/2]}}\int_{T_1}^{T_2} qT^{[2\Gamma/\gamma-3/2]}dT. \qquad \text{(A2.4)}$$

For water vapor, substituting $q_{(H_2O)} = q_{s(H_2O)}(p/p_s)^\lambda$ (where λ is a constant that varies with latitude, following OA), using (A2.3) and integrating, yields

$$u_{(H_2O)}[T_2,T_1]=\frac{c_0p_s}{R\gamma}\frac{q_{s(H_2O)}}{T_s^{[\Gamma/\gamma(2+\lambda)-1/2]}}\int_{T_1}^{T_2} T^{[\Gamma/\gamma(2+\lambda)-3/2]}dT$$
$$=\frac{c_0p_s}{R\gamma}\frac{q_{s(H_2O)}}{[\Gamma/\gamma(2+\lambda)-1/2]}\left(\frac{T}{T_s}\right)^{[\Gamma/\gamma(2+\lambda)-1/2]}\Bigg|_{T_1}^{T_2}. \qquad \text{(A2.5)}$$

For carbon dioxide, $q_{(CO_2)} \equiv q_{s(CO_2)}$ is constant with altitude. Therefore, integration of (A2.4) gives

$$u_{(CO_2)}[T_2,T_1]$$
$$=\frac{c_0p_s}{R\gamma}\frac{q_{s(CO_2)}}{[2\Gamma/\gamma-1/2]}\left(\frac{T}{T_s}\right)^{[2\Gamma/\gamma-1/2]}\Bigg|_{T_1}^{T_2}. \qquad \text{(A2.6)}$$

REFERENCES

Budyko, M. I., 1969: The effect of solar radiation variations on the climate of the earth. *Tellus,* **21,** 611–619.

Cess, R. D., 1974: Radiative transfer due to atmospheric water vapor: Global considerations of the earth's energy balance. *J. Quant. Spectrosc. Radial. Transfer.,* **14,** 861–871.

——, 1976: Climatic change: An appraisal of atmospheric feedback mechanisms employing zonal climatology. *J. Atmos. Sci.,* **33,** 1831–1843.

Ellis, J. S., and T. H. Vonder Haar, 1976: Zonal average earth radiation budget measurements from satellites for climate studies. *Atmos. Sci. Pap. 240,* Colorado State University.

Elsasser, W. M., and M. F. Culbertson, 1960: Atmospheric radiation tables. *Meteor. Monogr.,* **4,** No. 23, 43 pp.

Gruber, A., and A. F. Krueger, 1984: The status of the NOAA outgoing longwave data set. *Bull. Amer. Meteor. Soc.,* **65,** 958–962.

Harshvardhan, and J. A. Weinman, 1982: Infrared radiative transfer through a regular array of cuboidal clouds. *J. Atmos. Sci.,* **39,** 431–439.

Hartmann, D. L., and D. A. Short, 1979: On the role of zonal asymmetries in climate change. *J. Atmos. Sci.,* **36,** 519–528.

Kasahara, A., and W. W. Washington, 1971: General circulation experiments with a six-layer NCAR model, including orography, cloudiness and surface temperature calculations. *J. Atmos. Sci.,* **28,** 657–701.

London, J. L., 1957: *A Study of the Atmospheric Heat Balance. Final Report.* Contract AF 19(122)-165, College Eng., New York University, 99 pp. [NTIS NO. PB115626].

Manabe, S., 1969: Climate and the ocean circulation. I: The atmospheric circulation and the hydrology of the earth's surface. *Mon. Weather Rev.,* **97,** 739–774.

——, and R. T. Wetherald, 1967: Thermal equilibrium of the atmosphere with a given distribution of relative humidity. *J. Atmos. Sci.,* **24,** 241–259.

Neeman, B. U., 1986a: The modeling of basic feedback processes and some experiments with a coupled climate–ice sheet model: Application to the Milankovitch theory and climate sensitivity. Ph.D. thesis, Tel-Aviv University, 256 pp.

——, J. H. Joseph and G. Ohring, 1986b: A vertically integrated snow/ice model over land/sea for climate models: Impact on orbital change experiments. (submitted to *J. Geophys. Res.*)

——, —— and ——, 1986c: A parameterization of eddy exchange coefficients: Application to a dynamic climate model. (in preparation).

——, G. Ohring and J. H. Joseph, 1986d: The Milankovitch theory and climate sensitivity. I: Equilibrium climate model solutions for the present surface conditions. (submitted to *J. Geophys. Res.*)

North, G. R., R. F. Cahalan and J. A. Coakley, Jr., 1981: Energy balance climate models. *Rev. Geophys. Space Phys.,* **19,** 91–121.

Ohring, G., and S. Adler, 1978: Some experiments with a zonally averaged climate model. *J. Atmos. Sci.,* **35,** 186–205.

——, and ——, 1980: The annual climatic cycle: simulations and sensitivity studies with a zonally averaged model. *Extended Abstracts, International Radiation Symposium,* Colorado State University, Fort Collins, 277–279.

——, and A. Gruber, 1984: Satellite radiation observations and climate theory. *Adv. Geophys.,* **25,** 237–304.

Oort, A. H., and E. M. Rasmusson, 1971: Atmospheric Circulation Statistics, *NOAA Prof. Pap. No. 5,* U.S. Dept. of Commerce.

Ramanathan, V., L. B. Callis and R. E. Boughner, 1976: Sensitivity of surface temperature and atmospheric temperature to perturbations in the stratospheric concentration of ozone and nitrogen dioxide. *J. Atmos. Sci.*, **33,** 1092–1112.

Sasamori, T., 1968: The radiative cooling calculation for application to general circulation experiments. *J. Appl. Meteor.*, **7,** 721–729.

——, 1970: Simplification of radiative cooling calculation for application to atmospheric dynamics. WMO Tech. Note 104, 479–488.

Short, D. A., G. R. North, T. D. Bess and G. L. Smith, 1984: Infrared parameterization and simple climate models. *J. Appl. Meteor.*, **23,** 1222–1233.

Simmonds, I., and C. Chidzey, 1982: The parameterization of long-wave flux in energy balance climate models. *J. Atmos. Sci.*, **39,** 2144–2151.

Wang, W. C., W. B. Rossow, M. S. Yao and M. Wolfson, 1981: Climate sensitivity of a one-dimensional radiative-convective model with cloud feedback. *J. Atmos. Sci.*, **38,** 1167–1178.

Warren, S. G., and S. H. Schneider, 1979: Seasonal simulation as a test for uncertainties in the parameterizations of a Budyko-Sellers zonal climate model. *J. Atmos. Sci.*, **36,** 1377–1391.

Winston, J. S., A. Gruber, T. I. Gray, Jr., M. S. Varnadore, C. L. Earnest and L. P. Manello, 1979: *Earth–atmosphere radiation budget analyses derived from NOAA satellite data, June 1974–February 1978.* Vols. 1 and 2, NOAA, NESS.

Yamamoto, G., 1952: On a radiation chart. *Sci. Rep. of the Tohoku Univ.*, Series 5, **4,** 9–23.